Single-Photon Ionization Mass Spectrometry Using a Vacuum Ultraviolet Femtosecond Laser

Phan, Thang Dinh
Division of International Strategy, Center of Future Chemistry, Kyushu University

Li, Adan
Division of International Strategy, Center of Future Chemistry, Kyushu University

Nakamura, Hiroshi
Division of International Strategy, Center of Future Chemistry, Kyushu University

Imasaka, Tomoko
Department of Environmental Design, Graduate School of Design, Kyushu University

他

KYUSHU UNIVERSITY

Single Photon Ionization Mass spectrometry Using a Vacuum Ultraviolet Femtosecond Laser

Thang Dinh Phan,[†] Adan Li,[†‡] Hiroshi Nakamura,[†] Tomoko Imasaka,[§*] and Totaro Imasaka[†#]

[†]Division of International Strategy, Center of Future Chemistry, Kyushu University, 744 Motooka, Nishi-ku, Fukuoka 819-0395, Japan

[‡]College of Environmental and Chemical Engineering, Yanshan University, Qinhuangdao 066004, China

[§]Department of Environmental Design, Graduate School of Design, Kyushu University, 4-9-1, Shiobaru, Minami-ku, Fukuoka 815-8540, Japan

[#]Hikari Giken, Co., 2-10-30, Sakurazaka, Chuou-ku, Fukuoka 810-0024, Japan

* To whom correspondence should be addressed. E-mail: imasaka@design.kyushu-u.ac.jp

Keywords: Single photon ionization, Time-of-flight mass spectrometry, Vacuum ultraviolet, Femtosecond laser, Amino polycyclic aromatic hydrocarbon, Nonlinear optics

ABSTRACT: The wavelength of a femtosecond Ti:sapphire laser (TS, 800 nm) was converted into the ultraviolet (UV, 200 nm) using three beta-barium borate crystals (β-BaB$_2$O$_4$) for frequency doubling and subsequent mixing. The UV pulse was further converted into the vacuum ultraviolet (VUV, 185 nm) based on four-wave Raman mixing, in which a two-color pump beam consisting of the fundamental beam (800 nm) of the TS and the signal beam of an optical parametric amplifier (1200 nm) pumped by the TS was focused onto a capillary waveguide filled with hydrogen gas for molecular phase modulation and the single-color UV probe beam (200 nm) was then focused onto the waveguide for frequency modulation to generate anti-Stokes and high-order Stokes Raman sidebands at wavelengths of 185 nm and 218-267 nm, respectively. The efficiency of conversion from the UV (200 nm) to the VUV (185 nm) was 6 %. The ionization energy was calculated for thirteen amino polycyclic aromatic hydrocarbons using density functional theory, since they are associated with the development of occupational bladder cancers. The values calculated by the B3LYP/cc-pVDZ and ωB97Xd/cc-pVTZ methods were 6.24-7.14 eV (199-174 nm) and 6.41-7.35 eV (194-169 nm), respectively. A sample containing a mixture of 9-aminoanthracene, 3-aminofluoranthene, and 1-aminopyrene was separated by gas chromatography (GC), and the eluents were ionized with the VUV pulse (0.015 µJ) in mass spectrometry (MS). The analytes were observed on a two-dimensional display of GC/MS, and the detection limit obtained by single-photon ionization of 3-aminofluoranthene was 1 ng/µL.

Mass spectrometry (MS) is utilized in various fields, including the environmental and forensic sciences. The technique is in widespread use because of its excellent sensitivity and selectivity, permitting trace analysis of organic compounds in an actual sample containing numerous matrix species. Several techniques can be employed for ionization in MS but electron ionization is the most frequently used technique. However, a high-energy electron (e.g. 70 eV) sometimes causes the analyte molecule to dissociate, thus preventing the observation of a molecular ion, making identification and structural analysis more difficult. Several techniques such as chemical ionization or field ionization have been developed for observing a molecular ion. However, these techniques all have advantages and disadvantages as well. For example, matrix-assisted laser desorption ionization is useful for this purpose,[1] but it is difficult to combine it with a separation technique such as gas chromatography (GC) or liquid chromatography (LC). Although electrospray ionization can be combined with a separation technique such as LC,[2] it provides many multiply-charged ions, making the identification and structural analysis of a compound difficult.

A photoionization technique has been developed to solve the problem, since the ionization process can be controlled by changing the properties of the light source. In fact, this technique provides a useful means for soft ionization, and a molecular ion can, in most cases, be observed. There are a few approaches to this technique, as shown in Figure 1. A near-infrared (NIR) laser can be used for multiphoton ionization (MPI), which can be directly used without a device for frequency conversion. On the other hand, an ultraviolet (UV) laser can be used for two-photon ionization (2PI) and the efficiency can be significantly improved when the first photon is used for excitation and the subsequent photon for ionization.[3-5] This scheme, referred to as resonance-enhanced two-photon ionization (RE2PI) or more generally as resonance-enhanced multiphoton ionization (REMPI), is preferred for efficient and selective ionization. However, the light source becomes more complicated, since a device for frequency conversion is necessary. A vacuum ultraviolet (VUV) photon allows single-photon ionization (SPI).[6-8] This technique has been combined with GC for trace analysis of organic compounds, in which the third harmonic emission (10.5 eV or 118 nm) of the third harmonic beam (3.50 eV or 355 nm) of a Nd:YAG laser (1.1 eV or 1064 nm) has successfully been utilized.[9] A synchrotron radiation source has also been employed as a tunable VUV light, although the system becomes more complicated.[10,11] VUV emission from a microdischarge has been employed as the ionization source in MS and applied to a GC detector.[12] A conventional VUV lamp is useful for practical applications,[13] although the volume of the ionization region cannot be decreased, making combining it with a separation technique more difficult.

A femtosecond laser was recently employed for the ionization of organic compounds[14] and has been combined with gas chromatography for practical trace analysis.[15] There are two approaches, i.e., NIR and UV ionizations. The former is simple and the ionization efficiency can be substantially improved in NIR-MPI by reducing the width of the laser pulse. However, it sometimes suffered from dominant fragmentation. The latter is a more complicated system and the pulse energy decreases by the use of a frequency converter. However, it provides a molecular ion in most cases and has been successfully used even for a molecule, the lifetime of which is shortened by internal conversion and intersystem crossing, e.g., polychlorinated polycyclic aromatic hydrocarbons (PAHs) such as dioxins,[16] polychlorinated/polybrominated biphenyls,[17,18] and nitro aromatic hydrocarbons.[19] It should be noted that non-resonant two-photon ionization (NR2PI) must be used to reduce the excess energy in the ionic state to prevent fragmentation when a molecule cannot be excited using two photons with half of the ionization energy. The efficiency of ionization can, however, be improved to a level of RE2PI by increasing the peak power and then decreasing the pulse width of the laser.[20] This is a distinct advantage of femtosecond UV ionization for observing a molecular ion. To our knowledge, studies concerning the analytical use of a femtosecond VUV laser as the ionization source in SPI MS has not been reported.

Amino polycyclic aromatic hydrocarbons (APAHs) are utilized as intermediate compounds for organic synthesis of azo dyes which are widely used for coloring textile products and have been produced since the 1920s. However, some APAHs have been reported to stimulate the development of occupational bladder cancers. For example, large amounts of 2-naphthylamine were produced in the 1950s but its production has been prohibited since 1972 in Japan.[21] More recently, the Ministry of Health, Labor and Welfare, Japan reported that cases of occupational bladder cancer were identified in several workers who were handling *o*-toluidine in 2015.[22] These aromatic amines are reported to have low ionization energies (6.87-7.87 eV), due to the lone pair electrons on the nitrogen atom in the molecule.[23]

There are many approaches to generate an ultrashort optical pulse in the UV-VUV region based on nonlinear optical phenomena. A femtosecond pulse at 200 nm has been produced by the fourth harmonic generation of a femtosecond Ti:sapphire laser (800 nm) and is used as the ionization source in MS to determine pesticides in vegetables.[24,25] However, generating a pulse below 200 nm becomes more difficult because of the limited transparency and phase mismatching of a nonlinear optical crystal in the VUV region.[26-28] Four-wave mixing (FWM) in a rare gas has been employed for the frequency conversion of the NIR femtosecond pulse to generate a VUV pulse at 160 nm.[29] The

wavelength of the VUV pulse was tuned in the 146-151 nm range using a tunable NIR femtosecond laser.[30] The efficiency of conversion can be improved by employing a resonant transition process. When a hydrogen molecule is used as a nonlinear medium, the laser wavelength can be shifted by 4155 cm^{-1} toward longer or shorter wavelengths based on four-wave Raman mixing (FWRM).[31] In fact, a two-color pump beam (800 and 1200 nm) was focused onto hydrogen in a gas cell for molecular phase modulation, and a single-color probe beam (267 nm) was introduced into the cell for frequency modulation to generate the first and second anti-Stokes Raman sidebands (240 and 300 nm, respectively).[32] These UV pulses have been employed as the ionization source for the determination of explosives by MS.[33] The wavelength can be extended to the VUV region by using a probe beam at 200 nm, providing anti-Stokes emission at 185 nm (6.70 eV).[34] The efficiency of frequency conversion was estimated to be 11% at the region where the probe beam was spatially overlapped with the focused pump beam.[35] However, the efficiency of conversion of the total probe beam was much less than 1%. This VUV pulse has not yet been used in analytical spectroscopy.

In this study, we report on the generation of a VUV femtosecond optical pulse by focusing a two-color pump beam (800 and 1200 nm) and a single-color probe beam (200 nm) onto hydrogen gas in a capillary waveguide for spatial mode matching and extending the interaction length of the laser beam and the nonlinear optical medium to improve conversion efficiency. The VUV pulse (185 nm) generated by FWRM was employed as the ionization source in MS to determine APAHs that were separated by GC. We discuss the advantages and limitations of this method for potential applications to practical trace analysis.

EXPERIMENTAL SECTION

Apparatus. Figure 2 shows a block diagram of the experimental apparatus used in this study, which consists of two parts for the generation of an ultrashort VUV pulse and for use as an ionization source in MS.

Generation of a UV pulse. As shown in Figure 2A, a fundamental beam of a Ti:sapphire laser (800 nm, 35 fs, 3.6 W, 1 kHz, Legend Elite, Coherent) was used as a pump source for an optical parametric amplifier (OPA, OPerA Solo, Coherent). The transmitted beam (800 nm, 610 mW) from the last stage of the OPA was employed as one of the components for a two-color pump beam. The signal beam of the OPA (1200 nm, 320 mW) was passed through a half-wave plate (λ/2-1) to rotate the direction of polarization so as to be parallel to the beam at 800 nm for use as the other component

of the two-color pump beam. Timing of the pulse was adjusted using a time delay (TD-1). The two beams were combined using a dichroic mirror (DM-1) and were focused using a concave mirror (CM, focal length 750 mm, aluminum, Sigma Koki) onto a capillary waveguide (inner diameter 140 μm, length 250 mm) placed in a gas cell with CaF_2 windows (thickness of 0.5 mm). The cell was filled with hydrogen gas, and the pressure was measured using a pressure meter (AP44, Keyence). The frequency separation of the two beams was adjusted to the vibrational energy (4155 cm^{-1}) of the molecular hydrogen used as a nonlinear optical medium for molecular phase modulation: a hydrogen molecule can be prepared at the vibrationally excited level on the ground state by excitation at 800 nm and a subsequent stimulation transition at 1200 nm. The remaining part (800 nm, 1.6 W) from the OPA for UV frequency conversion (not used in this study) was passed through a β-barium borate crystal (BBO-1, $\theta = 29.2º$, $\phi = 0º$, $\Delta t = 0.2$ mm) to generate the second harmonic emission (400 nm, 600 mW). The beam was passed through a time plate (TP) composed of α-BaB$_2$O$_4$, which was used for a time delay of the 800-nm pulse to temporally overlap with the 400-nm pulse, and a half wave plate (λ/2-2) to adjust the direction of polarization to be parallel to each other. The beams were introduced into a β-barium borate crystal (BBO-2, $\theta = 44.3º$, $\phi = 0$ º, $\Delta t = 0.1$ mm) to generate the third harmonic emission (267 nm, 120 mW, 45 fs) by sum frequency mixing, which was separated by a dichroic mirror (DM-2) and then recombined by a dichroic mirror (DM-3) with the fundamental beam (800 nm, 900 mW) after passing it through a half wave plate (λ/2-3) to change the direction of polarization to be parallel to the third harmonic emission. The output power at 1200, 800, 400, and 267 nm was measured using a power meter (FieldMaxII-TO, Coherent). These pulses were temporally overlapped with each other using a time delay (TD-2). The recombined beam was passed through a β-barium borate crystal (BBO-3, $\theta = 35º$, $\Delta t = 0.15$ mm) to generate the fourth harmonic emission (200 nm, 10 mW) by sum frequency mixing. The output power at 200 nm was measured using a power meter (J3-09, Molectron).

Generation of a VUV pulse. The fourth harmonic emission was isolated using a dichroic mirror (DM-4) and was passed through a time delay (TD-3). After being combined with the two-color pump beam (800, 1200 nm) using a dichroic mirror (DM-5), the probe beam was focused onto the capillary waveguide for frequency modulation, generating Stokes (218 nm) and anti-Stokes (185 nm) emissions at longer and shorter wavelengths, respectively. The time delay (TD-3) was optimized to generate the maximum intensities for the Stokes and anti-Stokes emissions.[32] The VUV spectrum was measured using a multichannel spectrometer (Maya2000-Pro, Ocean Optics). The space inside the

spectrometer and the interface section between the spectrometer and the gas cell were purged with nitrogen gas supplied from a cylinder.

Mass spectrometer. The gas cell was directly combined with a vacuum chamber evacuated at below 1 Pa to reduce the absorption of the VUV emission by ambient air, as shown in Figure 2B. The beam from the capillary waveguide was focused using a concave mirror (CM, aluminum, focal length 500 mm, Sigma Koki) mounted on a vacuum-tight angle-changeable holder onto a laboratory-made MS (HG-1, Hikari Giken, Fukuoka, Japan).[36,37] A wedged substrate (thickness 5 mm, fused silica, angle 2º, Sigma Koki) was inserted in the beam path to separate the NIR beams, although it slightly expands the pulse width. Note that there are several pulse compression techniques in the near-UV/visible/NIR region such as chirped mirror and a grating/prism pair. However, none of them can be used in the UV/VUV region. A sample of pentachlorobenzene was continuously introduced into the MS to optimize the experimental conditions. This procedure was not applied in the case of the APAHs to avoid health hazard arising from their carcinogenicity.

Gas chromatograph. A sample mixture was injected into a GC (6890N, Agilent Technologies), and analytes were separated using a DB-5ms column (length 30 m, inner diameter 0.25 mm, film thickness 0.25 μm). The temperature program of the GC oven was as follows; initial temperature 60 °C hold for 1 min, a rate of 40 °C/min to 200 °C, then 20 °C/min to 280 °C hold for 6 min. Helium was used as a carrier gas, and the flow rate was adjusted at 1 mL/min. The amount of sample injected into the GC was 1 μL. The ions induced by a laser pulse was detected using a microchannel plate detector (F4655-11, Hamamatsu Photonics). The signal was recorded by a digitizer (Acqiris AP240, Agilent Technologies), and two-dimensional data of GC-MS was constructed using a home-made software programmed by the Visual Basic.

Samples. A sample of pentachlorobenzene was purchased from Tokyo Chemical Industry. The 3-aminofluoranthene (3-AFLU, 90%) and 1-aminopyrene (1-APYR, 97%) samples were obtained from Sigma-Aldrich and 9-aminoanthracene (9-AANT, 96%) from Angene International Limited. A sample mixture containing 100 or 3.3 ng/μL for each compound was prepared by dissolving these chemicals in ethanol.

Quantum Chemical Calculations. The number of ionization energies reported for APAHs in the database is limited especially for large toxic/carcinogenic compounds because of the health hazard in the experiment, although they are more important in practical trace analysis Then, quantum chemical calculations were performed to examine the ionization mechanism using a Gaussian16

program series package. The optimized geometries and the harmonic frequencies were calculated based on density functional theory (DFT) using the B3LYP method with a cc-pVDZ basis set.[38] Vertical ionization energy was evaluated from the difference between the energies of the ground and ionic states at the levels of B3LYP/cc-pVDZ and ωB97XD/cc-pVTZ. The lowest 40 singlet transition energies and the oscillator strengths were calculated using time-dependent DFT at levels of B3LYP/cc-pVDZ and ωB97XD/cc-pVTZ, and the predicted absorption spectra were generated using the Gauss View 5 software program by assuming a Gaussian-profile peak with a full width at half maximum of 0.333 eV for each transition.

RESULTS AND DISCUSSION

Generation of a VUV pulse. Figure 3 shows a photograph recorded by projecting the Raman emission on a white screen after passing it through a fused silica prism. Multi-color emissions were observed from the fourth anti-Stokes (342 nm) to the first anti-Stokes (600 nm) when the probe beam (200 nm) was interrupted in the experiment. These Raman sidebands (340-400 nm) were then generated by two-color FWRM. As shown in Figure S1, the intensity of the emission decreased rapidly for higher-order anti-Stokes Raman sidebands. Therefore, it was difficult to generate VUV emission based on two-color FWRM. On the other hand, multi-color emissions were observed from the first anti-Stokes (185 nm) to the third Stokes (267 nm) by introducing the probe beam (200 nm), indicating that they are generated by three-color FWRM. Figure 4 shows the spectrum of the Raman sidebands measured using a VUV spectrometer. The intensity of the anti-Stokes emission was equal to that of the first Stokes emission, suggesting that these sidebands were generated via FWRM: only the Stokes emission is pronounced in the stimulated Raman scattering. The dependence of the pressure of the hydrogen gas on the intensity of the VUV emission (185 nm) is shown in Figure S2. The optimal value was observed at 1.8 atm, indicating that phase matching is required and the anti-Stokes emission is then generated via FWRM. The ratio of the Raman sidebands and the probe beam transmitted from the waveguide was 6 %. The pulse energy of the 200-nm beam was 4 μJ at the entrance window of the gas cell. By taking the transmission and reflection efficiencies of the window (90%), the capillary (12%), and the mirror (85%) into account, the pulse energy in the MS was estimated to be $4 \times 0.9 \times 0.12 \times 0.9 \times 0.85 \times 0.85 \times 0.9 = 0.25$ μJ. The pulse energy of the 185-nm emission can then be estimated to be $0.25 \times 0.06 = 0.015$ μJ. When the multi-color emission was separated by wedged substrates, the VUV emission at 185 nm could be visually confirmed at the exit window of the MS, as shown in Figure S3.

Spectral Properties. Table 1 shows the ionization energies calculated for pentachlorobenzene and thirteen APAHs. The ionization energies were 8.92 eV (139 nm) and 6.24 – 7.14 eV (199 – 174 nm), respectively, for these compounds, when the B3LYP/cc-pVDZ method was used (the values were slightly larger when the ωB97XD/cc-pVTZ method was used). The wavelength corresponding to 9-AANT, 3-AFLU, and 1-APYR were 191, 182, and 190 nm, respectively. The ionization energy reported for 1-APYR in the NIST database was 6.8 eV (182 nm), which was much lower than the value of 9.11 – 9.21 eV (136 – 135 nm) reported for pentachlorobenzene: no data are available for 9-AANT and 3-AFLU.[39] These results suggest that APAHs can be potentially ionized using a single photon at 185 nm. The absorption spectra calculated for these compounds are shown in Figure S4. Pentachlorobenzene can be ionized via NR2PI at 267 nm. It is, however, difficult to ionize using a single photon at 185 nm. On the other hand, APAHs can be ionized via RE2PI at around 370 nm and can be single-photon ionized at around 185 nm. The ionization scheme summarized in Figure 5 suggests that two additional photons at 800 nm are needed to ionize pentachlorobenzene using the VUV pulse at 185 nm. On the other hand, APAHs have the potential to be single-photon ionized at 185 nm or can be ionized with an additional NIR photon (800 nm) at 200 or 218 nm. Note that the values obtained by DFT depend on the method used for the calculation (see Table 1) and cannot accurately be predicted (error, ca. 0.2 eV). The calculated values should therefore be used only for semi-quantitative discussion.

Pentachlorobenzene. Pentachlorobenzene was used as a reference compound to compare the ionization mechanism with the APAHs. Figure 6 shows the mass spectrum in the region where a molecular ion appears. Several molecular ion isotopomers with different numbers of ^{35}Cl and ^{37}Cl atoms were clearly observed. Note that the noise arising from the intensity fluctuation of the VUV pulse can be suppressed to negligible levels since the signal was accumulated 1000 fold to construct a mass spectrum. As shown in Figure 5 and Figure S4-A, the molecule would be ionized via RE2PI when the fourth harmonic emission (200 nm) was used for ionization. The signal intensity was increased by 1.5-fold when the Raman sidebands (185 and 218-nm) were generated. Since a photon energy even at 185 nm is insufficient for SPI (see Figure 5A), this signal enhancement can be attributed to two-photon ionization assisted by the 200-nm photon.

APAHs. A two-dimensional display for a sample mixture containing 9-AANT, 3-AFLU, and 1-APYR) is shown in Figure 7, which was measured in the presence of the VUV pulse (185 nm) in addition to the pulses at 200 and 218 nm. Molecular ions consisting of several isotopomers with ^{12}C

and ^{13}C atoms were observed at retention times of 7.59, 9.38, and 9.68 min for these compounds, respectively: other small signals are due to isomers present as impurities in the chemical reagents (e.g., PYR with an amino group substituted at different positions). Figure 8 shows chromatograms and mass spectra for a sample mixture measured at lower concentrations. The signal intensity was increased for 3-AFLU by introducing the VUV pulse at 185 nm. In contrast, the signal intensity of 1-APYR remained unchanged even when a VUV pulse was generated. The signal enhancement for 3-AFLU likely arises from SPI using a photon at 185 nm (6.70 eV). On the other hand, a photon energy at 185 nm would be insufficient (or inefficient) for 1-APYR and would mainly appear via 2PI using the photons at 200 nm. These data suggest that the accuracy of the DFT calculations is insufficient for discussing the difference in ionization efficiency among APAHs (see Table 1). The detection limit achieved for 3-AFLU was 1 ng/μL.

Advantages and Limitations. SPI using a VUV pulse is a liner process and the selectivity is determined only by the wavelength of the ionization source. This is in contrast to MPI, in which the selectivity is also determined by the intensity of the ionization source (e.g., the efficiency of non-resonant process is strongly enhanced by increasing the peak power and then by decreasing the pulse width of the ionization source).[40-42] Actually, APAHs have low ionization energies, and, as a result, they can be preferentially ionized in MS. When a VUV femtosecond laser is used for SPI, a variety of optical pulses generated at different wavelengths by several nonlinear processes can be simultaneously used for MPI. In fact, the optical system in this study permits femtosecond pulses at 185, 200, 218, 240, 267, 800, and 1200 nm to also be used, other wavelengths (e.g., 218, 240, 267, 300, 342, 400, 800, and 1200 nm) are also available using a probe beam at 267 nm.[32-35] Therefore, a wide variety of ionization schemes can be studied based on SPI and RE2PI/NR2PI (and RE3PI/NR3PI). This provides us an additional tool for examining the ionization mechanism (see Figure 5). The limitation of SPI in this study was the poor sensitivity in MS, since the energy of the VUV pulse was limited to <0.02 μJ. This result can be ascribed to multiple frequency conversion steps (OPA, FHG, FWRM) and to poor transmission and reflection efficiencies of the optical components used. Note that the transmission efficiencies of the capillary waveguide can be improved by using a capillary with an optimal inner diameter; a center part (70%) of the Gaussian beam can be introduced into the waveguide in theory by fitting the beam size with the inner diameter of the capillary. In addition, the transmission and reflection efficiencies can be significantly improved by reducing the number of optical components and by using anti-reflection-coating windows and highly-

reflective dichroic mirrors (five aluminum mirrors for reflecting the UV beam and two aluminum mirrors for reflecting the VUV beam were used in this study for analytical application).

Other VUV Femtosecond Light Sources. A VUV laser emitting at shorter wavelengths (<185 nm) would be desirable for more general applications, since the ionization energies of other organic compounds are in the range of 6.5 – 10 eV (191 – 124 nm). As described above, the VUV pulse at 160 nm (2.5 μJ) is generated using noncollinear difference-frequency FWM ($\omega_{VUV} = 2\omega_{TH} - \omega_{NIR}$) between the fundamental and third harmonics of a Ti:sapphire laser in argon.[29] A tunable VUV pulse across the spectral region of 146–151 nm (0.09 μJ) can be generated by using the signal beam of OPA in krypton and argon.[30] The third harmonic emission (133 nm, 9.3 eV) generated in a rare gas using the second harmonics (400 nm) of a Ti:sapphire laser (800 nm) would be preferred for more general use of this technique (although the selectivity would be decreased), the conversion efficiency of which would be significantly improved using a high-peak-power ultrashort laser pulse. In a previous study, we reported on the generation of a femtosecond VUV pulse at 154.2 nm and attributed this to stimulated emission in molecular hydrogen, which would be an alternative approach for use in SPI MS.[43]

CONCLUSIONS

A VUV femtosecond optical pulse (185 nm) was generated by three-color FWRM using a two-color pump beam (800 and 1200 nm) and a single-color probe beam (200 nm) produced by the fourth harmonics of a Ti:sapphire laser (800 nm). A sample mixture containing APAHs was analyzed by MS using the VUV pulse as the ionization source in MS. The signal intensity of 3-AFLU was significantly increased by introducing a 185-nm pulse, which was in contrast to 1-APYR providing no signal enhancement. These data suggest that selective ionization can be achieved by SPI MS. A VUV pulse with a larger pulse energy at shorter wavelengths would be preferential for more general use in trace analyses.

ASSOCIATED CONTENT
Supporting Information
The Supporting Information is available free of charge at ……………..

Supporting information provides emission spectrum of Raman sidebands (Fig. S1), the dependence of the hydrogen gas pressure on the signal intensity of the Raman sidebands (Fig. S2), spectrograph of Raman sidebands (Fig. S3), and absorption spectra calculated for pentachlorobenzene and APAHs (Fig. 4S).

AUTHOR INFORMATION

Corresponding Author

[*] E-mail: imasaka@design.kyushu-u.ac.jp

ORCID

Phan Dinh Thang: 0000-0002-2446-0453

Adan Li: 0000-0002-5803-2457

Hiroshi Nakamura: 0000-0001-9058-4908

Tomoko Imasaka: 0000-0002-2131-4995

Totaro Imasaka: 0000-0003-4152-3257

Notes:

The authors declare no competing financial interest.

REFERENCES

(1) Fenn, J. B.; Mann, M.; Meng, C. K.; Wong, S. F.; Whitehouse, C. M. Electrospray ionization for mass spectrometry of large biomolecules. *Science* **1989**, *246*, 64-71.

(2) Karas, M.; Hillenkamp, F. Laser desorption ionization of proteins with molecular masses exceeding 10,000 daltons. *Anal. Chem.* **1988**, *60*, 2299-2301.

(3) Lubman, D. M.; Kronick, M. N. Mass spectrometry of aromatic molecules with resonance-enhanced multiphoton ionization. *Anal. Chem.* **1982**, *54*, 660-665.

(4) Boesl, U.; Zimmermann, R.; Weickhardt, C.; Lenoir, D.; Schramm, D.-W.; Kettrup, A.; Schlag, E. W. Resonance-enhanced multi-photon ionization: A species-selective ion source for analytical time-of-flight mass spectroscopy. *Chemosphere* **1994**, *29*, 1429−1440.

(5) Gunzer, F.; Krüger, S.; Grotemeyer, J. Photoionization and photofragmentation in mass spectrometry with visible and UV lasers. *Mass Spectrom. Rev.* **2019**, *38*, 202–217.

(6) Butcher, D. J. Vacuum Ultraviolet radiation for single-photoionization mass spectrometry: A Review. *Microchem. J.* **1999**, *62*, 354-362.

(7) Cao, L.; Muhlberger, F.; Adam, T.; Streibel, T.; Wang, H. Z.; Kettrup, A.; Zimmermann, R. Resonance-enhanced multiphoton ionization and VUV-single photon ionization as soft and selective laser ionization methods for on-line time-of-flight mass spectrometry: Investigation of the pyrolysis of typical organic contaminants in the steel recycling process. *Anal. Chem.* **2003**, *75*, 5639-5645.

(8) Mullen, C.; Irwin, A.; Pond, B. V.; Huestis, D. L.; Coggiola, M. J.; Oser H. Detection of explosives and explosives-related compounds by single photon laser ionization time-of-flight mass spectrometry, *Anal. Chem.* **2006**, *78*, 3807-3814.

(9) Zimmermann, R.; Welthagen, W.; Gröger, T. Photo-ionisation mass spectrometry as detection method for gas chromatography: Optical selectivity and multidimensional comprehensive separations. *J. Chromatogr. A* **2008**, *1184*, 296–308.

(10) Zhou, Z.; Guo, H.; Qi, F. Recent developments in synchrotron vacuum ultraviolet photoionization coupled to mass spectrometry. *Trends Anal. Chem.* **2011**, *30*, 1400-1409.

(11) Kleeblatt, J.; Ehlert, S.; Holzer, J.; Sklorz, M.; Rittgen, J.; Baumgartel, P.; Schubert, J. K.;

Zimmermann, R. Investigation of the photoionization properties of pharmaceutically relevant substances by resonance-enhanced multiphoton ionization spectroscopy and single-photon ionization spectroscopy using synchrotron radiation. *Appl. Spectrosc.* **2013**, *57*, 860-872.

(12) Lopez-Avila, V.; Cooley, J.; Urdahl, R.; Thevis, M. Determination of stimulants using gas chromatography/high-resolution time-of-flight mass spectrometry and a soft ionization source. *Rapid. Commun. Mass Spectrom.* **2012**, *26*, 2714-2724.

(13) Wang, Y.; Jiang, J.; Hua, Lei.; Hou, K.; Xie, Y.; Chen, P.; Liu, W.; Li, Q.; Wang, S.; Li, H. High-pressure photon ionization source for TOFMS and its application for online breath analysis. *Anal. Chem.* **2016**, *88*, 9047−9055.

(14) Chekalin, S. V.; Golovlev, V. V.; Kozlov, A. A.; Matveyets, Yu. A.; Yartsev, A. P.; Letokhov, V. S. Femtosecond laser photoionization mass spectrometry of tryptophan-containing proteins. *J. Phys. Chem.* **1988**, *92*, 6855-6858.

(15) Imasaka, T. Gas chromatography/multiphoton ionization/time-of-flight mass spectrometry using a femtosecond laser. A*nal. Bioanal. Chem.* **2013**, *405*, 6907-6912.

(16) Chang, Y.-C.; Imasaka, T. Simple pretreatment procedure combined with gas chromatography/multiphoton ionization/mass spectrometry for the analysis of dioxins in soil samples obtained after the Tōhoku earthquake. *Anal. Chem.* **2013**, *85*, 349-354.

(17) Duong, V. T. T.; Duong, V.; Lien, N. T. H.; Imasaka, T.; Tang, Y.; Shibuta, S.; Hamachi, A.; Hoa, D. Q.; Imasaka, T. Detection of polychlorinated biphenyls in transformer oils in Vietnam by multiphoton ionization mass spectrometry using a far-ultraviolet femtosecond laser as an ionization source. *Talanta* **2016**, *149*, 275-279.

(18) Shitamichi, O.; Imasaka, T.; Uchimura, T.; Imasaka, T. Multiphoton ionization/mass spectrometry of polybrominated diphenyl ethers. *Anal. Methods* **2011**, *3*, 2322-2327.

(19) Tang, Y.; Imasaka, T.; Yamamoto, S.; Imasaka, T. Multiphoton ionization mass spectrometry of nitrated polycyclic aromatic hydrocarbons. *Talanta* **2015**, *140*, 109-114.

(20) Kouno, H.; Imasaka, T. The efficiencies of resonant and nonresonant multiphoton ionization in the femtosecond region. *Analyst* **2016**, *141*, 5274-5280.

(21) Matsushima, M.; Kuwabara, T. The history and the present conditions of the occupational

bladder cancer in our country (Japanese). *Jpn. J. Urology* **2012**, *104*, 569-578.

(22) https://www.nikkei.com/article/DGXLASDG18HB0_Y5A211C1CR8000/

(23) Farrell, P. G.; Newton, J. Ionization potentials of primary aromatic amines and aza-hydrocarbons. *Tetrahedron Lett.* **1966**, *45*, 5517-5523.

(24) Hashiguchi, Y.; Zaitsu, S.; Imasaka, T. Ionization of pesticides using a far-ultraviolet femtosecond laser in gas chromatography/time-of-flight mass spectrometry. *Anal. Bioanal. Chem.* **2013**, *405*, 7053-7059.

(25) Yang, X.; Imasaka, T.; Li, A.; Imasaka, T. Determination of hexachlorocyclohexane by gas chromatography combined with femtosecond laser ionization mass spectrometry. *J. Amer. Soc. Mass Spectrom.* **2016**, *27*, 1999-2005.

(26) Nakazato, T.; Ito, I.; Kobayashi, Y.; Wang, X.; Chen, C.; Watanabe, S. Phase-matched frequency conversion below 150 nm in $KBe_2BO_3F_2$. *Opt. Express* **2016**, *24*, 17149-17158.

(27) Kanai, T.; Kanda, T.; Sekikawa, T.; Watanabe, S.; Togashi, T.; Chen, C.; Zhang, C.; Xu, Z.; Wang, J. Watt-level tunable deep ultraviolet light source by a KBBF prism-coupled device. *J. Opt. Soc. Am. B* **2004**, *21*, 370-375.

(28) Silva, J. L.; Crespo, H. M.; Weigand, R. Generation of high-energy vacuum UV femtosecond pulses by multiple-beam cascaded four-wave mixing in a transparent solid. *Appl. Opt.* **2011**, *50*, 1968-1973.

(29) Ghotbi, M.; Beutler, M.; Noack, F. Generation of 2.5μJ vacuum ultraviolet pulses with sub-50 fs duration by noncollinear four-wave mixing in argon. *Opt. Lett.* **2010**, *35*, 3492-3494.

(30) Ghotbi, M.; Trabs, P.; Beutler, M.; Noack, F. Generation of tunable sub-45 femtosecond pulses by noncollinear four-wave mixing. *Opt. Lett.* **2013**, *38*, 486-488.

(31) Imasaka, T.; Kawasaki, S.; Ishibashi, N. Generation of more than 40 laser emission lines from the ultraviolet to the visible regions by two-color stimulated Raman effect. *Appl. Phys. B* **1989**, *49*, 389-392.

(32) Mori, Y.; Imasaka, T. Generation of ultrashort optical pulses in the deep-ultraviolet region based on four-wave Raman mixing. *Appl. Sci.* **2018**, *8*, 784.

(33) Hamachi, A.; Okuno, T.; Imasaka, T.; Kida, Y.; Imasaka, T. Resonant and nonresonant

multiphoton ionization processes in the mass spectrometry of explosives. *Anal. Chem.* **2015**, *87*, 3027-3031.

(34) Vu, D.; Nguyen, T. N.; Imasaka, T. Ro-vibrational revival of a wave-packet in molecular hydrogen by three-color four-wave Raman mixing. *Opt. Laser Technol.* **2017**, *88*, 184-187.

(35) Vu, D.; Dinh, T. P.; Imasaka, T. Ro-vibrational revival of the molecular hydrogen wave packet by a two-color pump in four-wave Raman mixing. *Opt. Laser Technol.* **2018**, *102*, 22-24.

(36) Matsumoto, J.; Nakano, B.; Imasaka, T. Development of a compact supersonic jet/multiphoton ionization/time-of-flight mass spectrometer for the on-site analysis of dioxin, Part I: Evaluation of basic performance. *Anal. Sci.* **2003**, *19*, 379-382.

(37) Matsumoto, J.; Nakano, B.; Imasaka, T. Development of a compact supersonic jet/multiphoton ionization/time-of-flight mass spectrometer for the on-site analysis of dioxin, Part II, Application to chlorobenzene and dibenzofuran. *Anal. Sci.* **2003**, *19,* 383-386.

(38) Bauernschmitt, R.; Ahlrichs, R. Treatment of electronic excitations within the adiabatic approximation of time dependent density functional theory. *Chem. Phys. Lett.* **1996**, *256*, 454-464.

(39) https://webbook.nist.gov/cgi/cbook.cgi?ID=C608935&Mask=20#Ion-Energetics

(40) Zakheim D. S.; Johnson, P. M. Rate equation modelling of molecular multiphoton ionization dynamics. *Chem. Phys.* **1980**, *46*, 263-272.

(41) Boesl, U. Multiphoton excitation and mass-selective ion detection for neutral and ion spectroscopy. *J. Phys. Chem.* 1991, 95, 2949-2962.

(42) Madunil, S. L.; Imasaka, T.; Imasaka, T. Resonant and non-resonant femtosecond ionization mass spectrometry of organochlorine pesticides. *Analyst* **2019**, *145*, 777-783.

(43) Dinh, T. P.; Vu, D.; Imasaka, T. Vacuum-ultraviolet stimulated emission generated via four-wave Raman mixing in molecular hydrogen. *Appl. Phys. B* **2019**, *125*, 128.

Table 1. Ionization Energies Calculated Using B3LYP/cc-pVDZ and ωB97XD/cc-pVTZ.

Method/Basis Set	B3LYP/cc-pVDZ		ωB97XD/cc-pVTZ	
Compound	Ionization Energy (eV)	Wavelength (nm)	Ionization Energy (eV)	Wavelength (nm)
pentachlorobenzene	8.92	139	9.21	135
1-aminonaphthalene	7.12	174	7.31	170
2-aminonaphthalene	7.14	174	7.35	169
5-aminoacenaphthene	6.75	184	6.94	179
2-aminofluorene	6.83	182	7.08	175
2-aminoanthracene	6.58	189	6.81	182
9-aminoanthracene (9-AANT)	6.48	191	6.65	187
3-aminophenanthrene	6.88	180	7.14	174
9-aminophenanthrene	6.97	178	7.18	173
3-aminofluoranthene (3-AFLU)	6.82	182	6.84	181
1-aminopyrene (1-APYR)	6.53	190	6.72	184
7-aminobenzo(a)anthracene	6.46	192	6.67	186
6-aminochrysene	6.67	186	6.92	179
6-aminobenzo(a)pyrene	6.24	199	6.41	194

Figure Captions.

Figure 1. Ionization schemes. NIR, UV, and VUV lasers can be used for multi-photon, two-photon, and single-photon ionizations, respectively.

Figure 2. Block diagram of the experimental apparatus used in this study. (A) Optical configuration for the generation and measurement of the VUV pulse. (B) Vacuum chamber and optical components for focusing the beam into the MS. M, aluminum mirror; CM, concave mirror; DM, dichroic mirror, BBO, β-BaB_2O_4 crystal; $\lambda/2$, half-wave plate; TP, time plate (α-BaB_2O_4 crystal); TD, time delay; CaF_2, windows made of calcium fluoride, WS, wedged substrate (cf. Caption of Figure S3 for WS-2).

Figure 3. Photograph recorded by projecting the beam from the capillary waveguide on a white screen containing a phosphor. The beam was passed through a fused-silica prism under atmospheric conditions. The two-color pump beam (800 and 1200 nm) and the Stokes beam (2400 nm) were not observed because of low sensitivity of the camera in the NIR region. Note that the VUV beam at 185 nm is attenuated by the fused-silica prism and the ambient air.

Figure 4. Spectrum of the emission from the capillary waveguide measured using the VUV spectrometer. The hydrogen pressure was adjusted at 1.8 atm.

Figure 5. Ionization schemes. (A) Pentachlorobenzene. (B) APAHs. The VUV pulse at 185 nm can potentially be used for SPI of APAHs. However, the UV pulses at 218 and 200 nm are insufficient for SPI and an additional photon is required for 2PI.

Figure 6. Mass spectra measured for pentachlorobenzene at (A) 200 nm (B) 185 + 200 + 218 nm. The chemical structure of pentachlorobenzene is shown in the figure.

Figure 7. Two-dimensional display measured for a sample mixture of 9-AANT, 3-AFLU, and 1-APYR. The chromatogram measured at m/z = 193 (9-AANT) and 217 (3-AFLU and 1-APYR) are shown at the top of the display, respectively, and the mass spectra measured at retention times of 7.59 (9-AANT) and 9.38 min (3-AFLU) are shown at the right-hand side, respectively. Sample concentration, 100 ng/μL for each chemical. Laser wavelength, 218 + 200 + 185 nm.

Figure 8. Data measured for APAHs at (A) (C) 200 nm and (B) (D) 185 + 200 + 218 nm. (A) (B) Chromatograms measured at m/z = 217 (3-AFLU and 1-APYR). (C) (D) Mass spectra measured at a retention time of 9.38 min (3-AFLU). Sample concentration, 3.3 ng/μL for each compound.
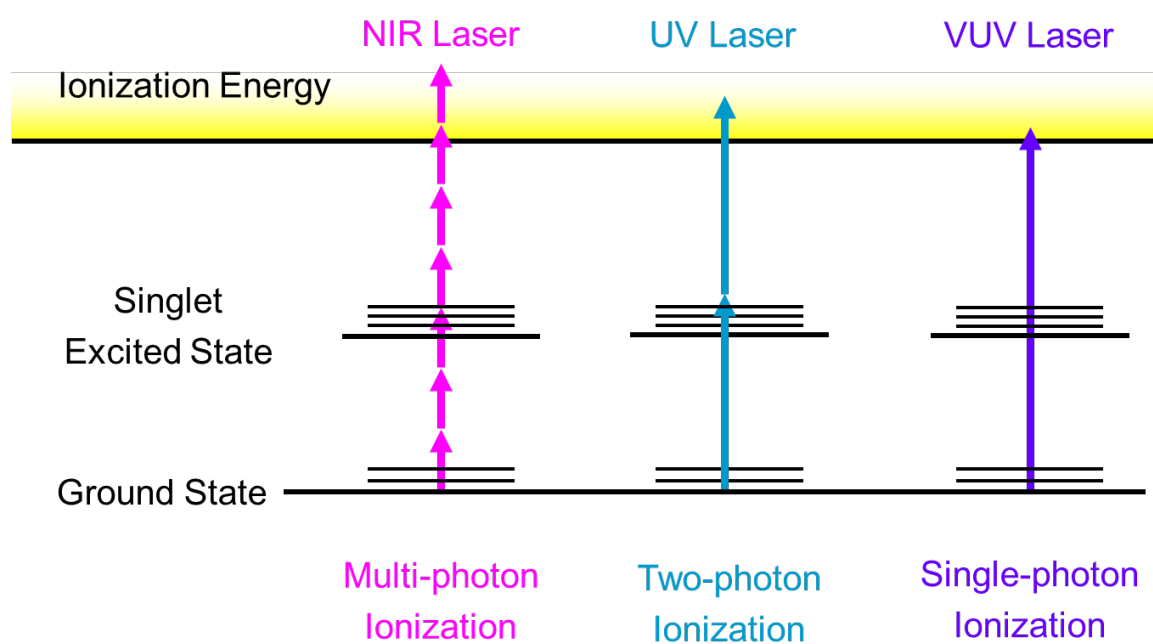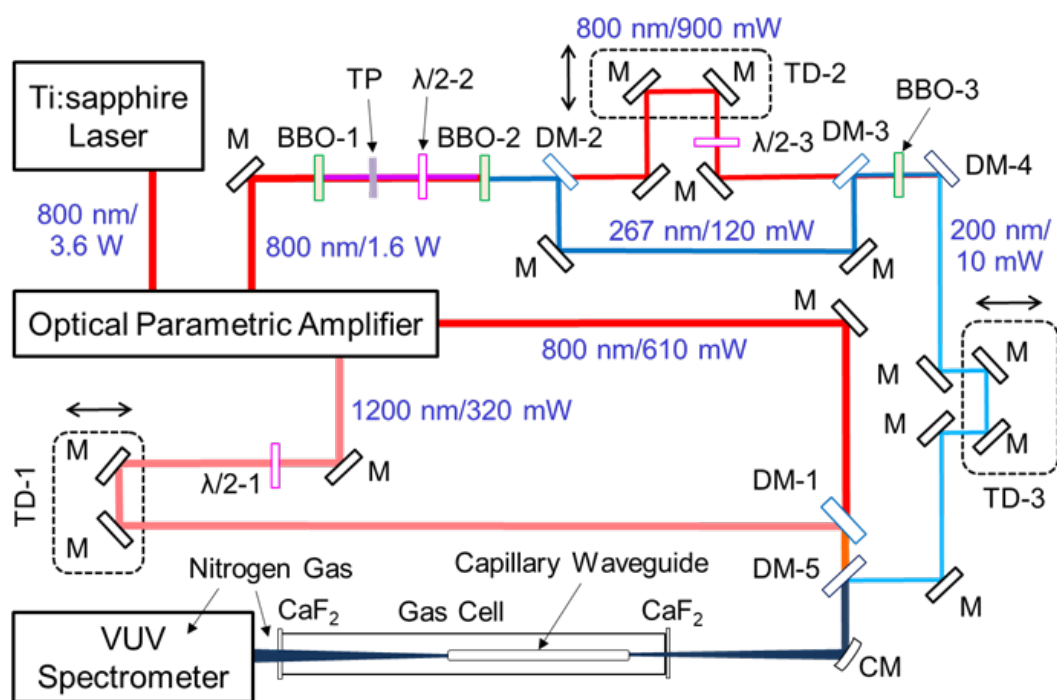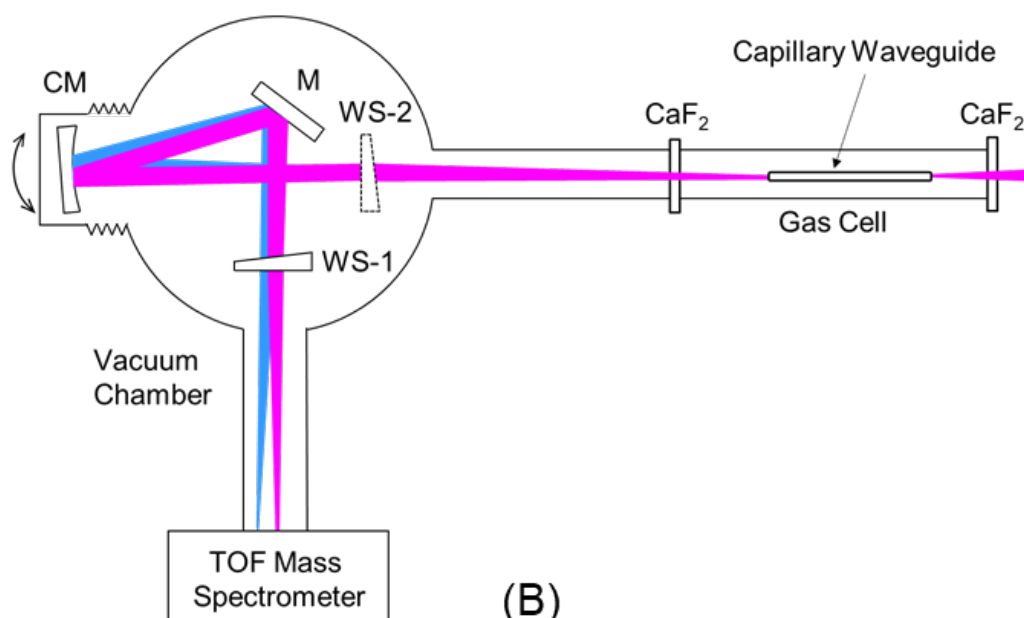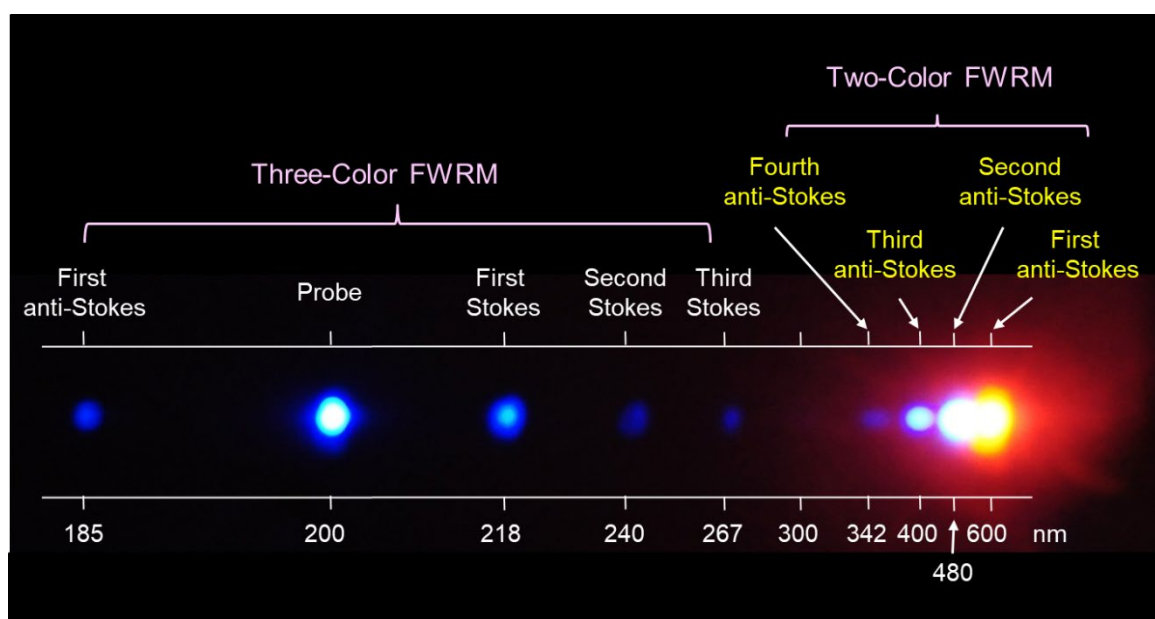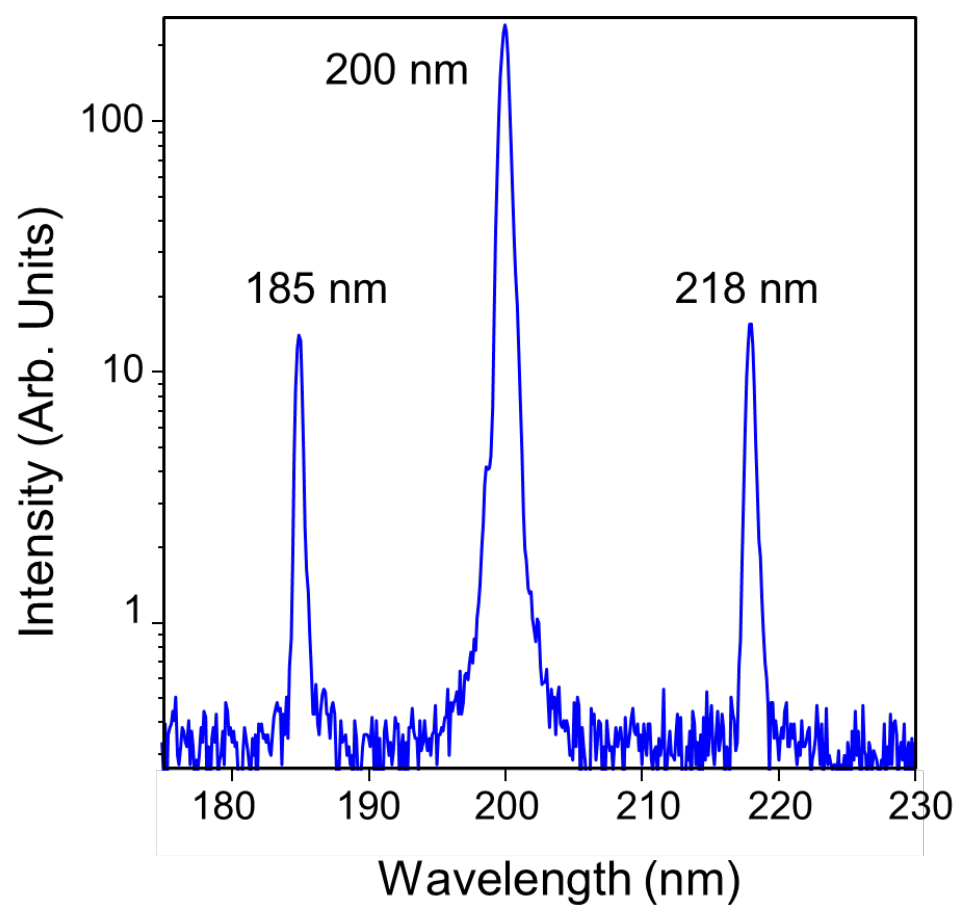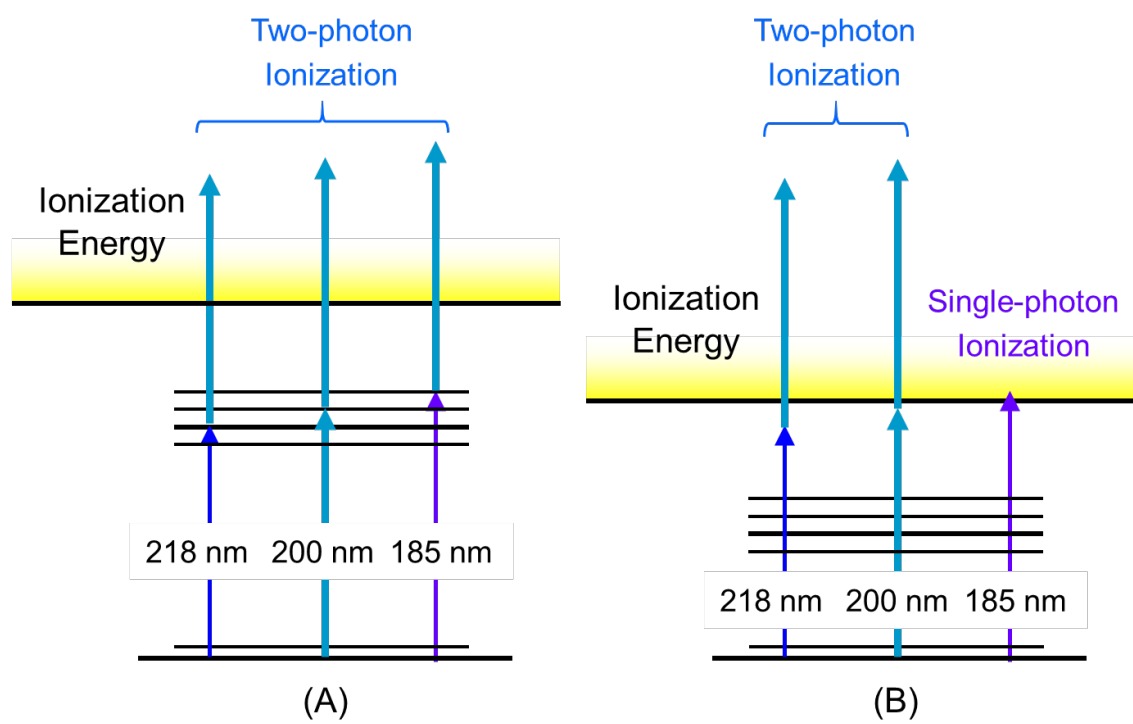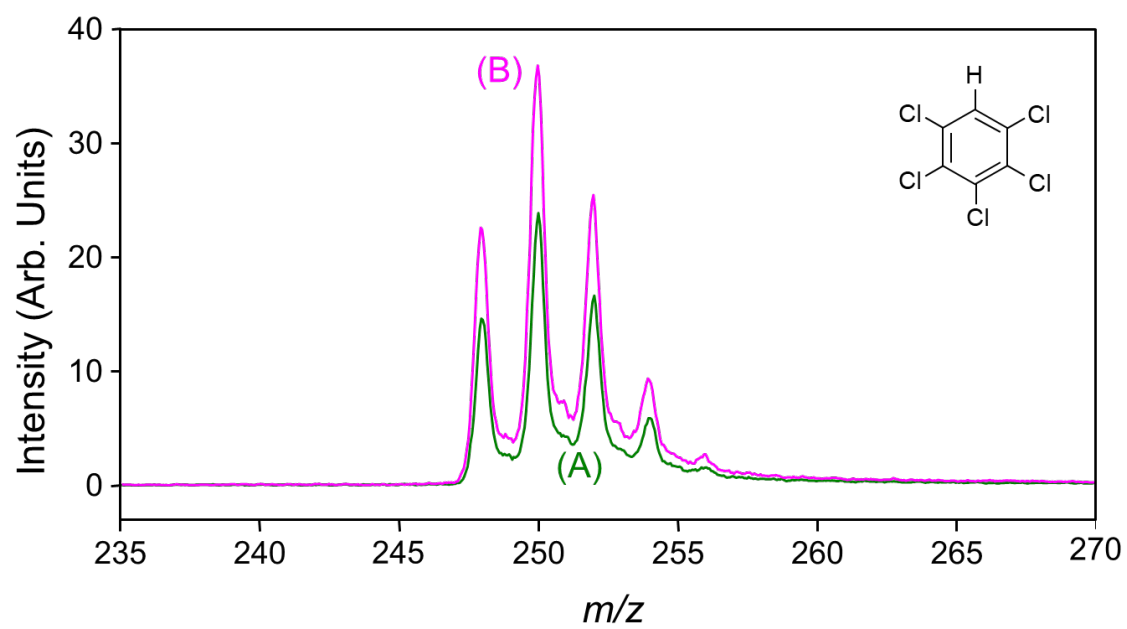
Figure 1

(A)

(B)

Figure 2

Figure 3

Figure 4

Figure 5

Figure 6

Figure 7

Figure 8

TOC